

Fairness-Aware Dynamic Electricity Pricing with Game-Theoretic Demand Response

You Wu^{1,*}, Suyash Devendra Sawant¹, and Aram Bahrini¹
*youw8@illinois.edu

¹Department of Business Administration
Gies College of Business
University of Illinois at Urbana-Champaign
Champaign, IL, USA

Abstract—Peak load stress on power grids continues to intensify as electrification accelerates, flexible loads such as electric vehicles proliferate, and demand becomes increasingly weather sensitive. Dynamic pricing can reduce peak demand, but pricing without explicit bounds can expose consumers to high bills during system stress. This paper proposes a price-bounded, threshold-based demand-response framework that limits elevated prices to hours when a day-ahead forecast signals grid strain, while limiting consumer exposure through both price ceilings and floors. We draw on publicly available data from the Pennsylvania–New Jersey–Maryland Interconnection load, market prices, and weather records to identify grid stress periods and train a 24-hour-ahead extreme gradient boosting load forecasting model with a Mean Absolute Percentage Error of 2.73% that drives pricing decisions. The pricing rule is deterministic, three-tier, and governed by explicit cap-and-floor constraints. We emphasize that demand response outcomes rest on assumed, uniform elasticity parameters and do not reflect observed consumer behavior. Historical simulations using Pennsylvania–New Jersey–Maryland Interconnection records from August 2025 through March 2026 show that, under these assumptions, the framework reduces peak-hour demand by 12.5% relative to flat rate pricing and lowers average consumer bills by 11.7% relative to time-of-use pricing. The bill advantage over time-of-use pricing widens progressively through the fall and winter months, driven more by the off-peak discount than by the stress hour premium, a distinction with implications for tariff design. Price bounds limit extreme prices and secondary peaks, producing smoother simulated demand shifts.

Index Terms—Dynamic electricity pricing, demand response, peak load reduction, load forecasting.

I. INTRODUCTION AND RELATED WORK

Electrification is increasing pressure on power systems, especially during peak-demand periods. As households and firms adopt electric vehicles and electric heating, system load becomes more difficult to manage during high-demand hours. At the same time, technologies such as EV chargers and programmable thermostats enable some users to shift their consumption in response to price signals. Weather shocks add further strain by pushing demand upward when the system is already tight.

Dynamic pricing is a common way to manage this problem. By varying retail electricity prices over time, utilities can encourage consumers to reduce or shift consumption away from high-stress periods. Prior studies show that well-designed demand response programs can reduce peak demand by 10–20% without materially reducing comfort or satisfaction [1], [2].

The difficulty is that dynamic pricing can also create bill risk when prices are not explicitly bounded. Consumers with limited flexibility, including shift workers, households without smart devices, and families with fixed heating or cooling needs, may bear a disproportionate share of peak-period costs. Extreme price spikes can impose substantial financial burdens on vulnerable households [3], [4]. The Electric Reliability Council of Texas crisis of February 2021 illustrated this risk clearly. Bill uncertainty and consumer distrust therefore remain major barriers to the wider adoption of dynamic tariffs [5].

Time-of-use (TOU) pricing divides the day into preset pricing periods, with rates fixed by hour and season [2]. Real-time pricing (RTP), by contrast, exposes consumers to hourly wholesale price variation and therefore provides a stronger signal, but also greater bill volatility [6]. Field evidence from the Pennsylvania–New Jersey–Maryland (PJM) region suggests that peak demand can fall by 10–30% under appropriately designed pricing incentives [1], [7].

A common way to model utility-consumer interaction under demand response is through a Stackelberg game. The utility sets the price, and consumers respond by adjusting usage. Yu et al. show that the operator’s optimal price depends on aggregate consumer elasticity [8], while Maharjan et al. study equilibrium behavior in smart-grid settings [9]. A recurring limitation in this literature is that prices are often left effectively unconstrained, allowing equilibrium outcomes that would be difficult to justify in practice. Borenstein [6] and Allcott [4] show that dynamic tariffs can disproportionately burden low-income and low-flexibility households, and later studies identify this distributional concern as a central adoption barrier [3], [5]. This issue matters here as well, because our framework also relies on a representative-consumer assumption with uniform elasticity. We retain that simplification for tractability, but return to its implications in Section VI. The

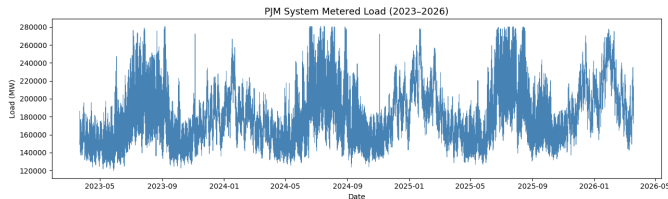


Fig. 1. PJM system metered load (2023–2026). The series exhibits pronounced summer and winter peaks, high-frequency daily cycles, and load ranging from approximately 120,000 to 281,000 MW across 25,990 cleaned hourly records.

main contribution of our approach is to impose hard bounds on the pricing rule in Section IV, thereby directly addressing the unconstrained-pricing problem.

Specifically, we propose a threshold-based pricing framework that raises prices only when next-day conditions indicate likely grid stress, rather than on a fixed daily schedule. The framework includes a price cap, a price floor, and a revenue-adequacy condition. We evaluate it using three years of PJM data and treat all demand-response results as simulated outcomes under assumed elasticity parameters, rather than as estimates of observed consumer behavior.

II. DATA SOURCES AND PREPROCESSING

A. PJM Load Data

We use hourly metered load data from the PJM Interconnection covering March 2023 to March 2026, obtained from PJM’s Data Miner portal. The raw dataset contains 789,120 zone-level records. We aggregate these observations across zones to construct a system-wide hourly load series. We then remove the top 1% of observations as data-quality artifacts. This trimming threshold was selected as the smallest cutoff that removed visually obvious meter-glitch spikes without discarding plausible demand extremes. The resulting cleaned dataset contains 25,990 hourly records, with a mean load of 183,434 MW, a standard deviation of 31,991 MW, and a range of 119,514–281,003 MW. Fig. 1 shows the full time series, including pronounced summer and winter peaks.

B. Weather and Market Data

Hourly weather observations for Philadelphia, PA were obtained from the Open-Meteo historical archive API. We use Philadelphia as a proxy for PJM’s service territory. This choice is reasonable but imperfect: Philadelphia lies near the geographic and population-weighted center of PJM’s Mid-Atlantic core, and its temperature series is more strongly correlated with aggregate PJM load over the training period than comparable series from Pittsburgh or Baltimore. At the same time, it likely understates heating-related demand in colder inland zones during winter stress events, which should be kept in mind when interpreting winter forecast performance. Weather variables include 2-meter temperature ($^{\circ}\text{C}$), relative humidity (%), 10-meter wind speed (km/h), and precipitation (mm).

Day-ahead locational marginal prices (DA-LMPs) at the system energy level were obtained from PJM’s day-ahead hourly

TABLE I
24-HOUR-AHEAD LOAD FORECAST PERFORMANCE (TEST SET)

Metric	Value
Mean Absolute Error (MAE)	5,340 MW
Root Mean Square Error (RMSE)	7,132 MW
Mean Absolute Percentage Error (MAPE)	2.73%
Average system load (test period)	191,411 MW
Training period	2023-03-29 → 2025-08-16
Test period	2025-08-16 → 2026-03-19

LMP files over the same period. DA-LMPs range from \$9.11 to \$1,501.14/MWh. Missing LMP values (approximately 3% of hours) were imputed using stratified mean imputation based on month, day of week, and hour of day. After merging the load, weather, and LMP data on a common hourly timestamp, the final dataset contains 25,990 records across 15 columns.

III. 24-HOUR-AHEAD LOAD FORECASTING

A. Model Design and Evaluation

Each hourly observation includes four feature groups: calendar variables (hour of day, day of week, month, and weekend flag); weather variables (temperature, relative humidity, wind speed, and a centered quadratic temperature term $(\text{temp} - \bar{\text{temp}})^2$ to capture the U-shaped relation between load and temperature); lagged load variables (lag_{24} , the load 24 hours earlier, and lag_{168} , the load one week earlier, which preserve a genuinely day-ahead forecasting setup); and day-ahead locational marginal price (DA-LMP), which provides forward-looking market information. After constructing the lagged variables and removing incomplete rows, 25,822 usable observations remain.

We train an eXtreme Gradient Boosting (XGBoost) model [11] using a strict temporal 80/20 train–test split. The training period spans 2023-03-29 to 2025-08-16 (20,657 hours), and the test period spans 2025-08-16 to 2026-03-19 (5,165 hours). The model uses 300 estimators, a maximum depth of 6, a learning rate of 0.05, a subsample ratio of 0.8, column subsampling of 0.8, and a random seed of 42. Table I reports out-of-sample performance.

Fig. 2 compares predicted and actual load over the first 30 days of the test period. The model tracks weekday ramps, weekend troughs, and late-summer afternoon peaks closely. A MAPE of 2.73% is consistent with day-ahead forecasting performance reported for large power systems [10], [11]. That summary measure, however, masks weaker performance during the winter holiday period from late December 2025 to early January 2026, when commercial and industrial shutdowns reduce load in ways that lag and calendar features do not fully capture. Although forecast errors are larger in MW terms during that interval, the effect on stress-hour classification is limited because holiday loads generally remain below the 229,127 MW stress threshold.

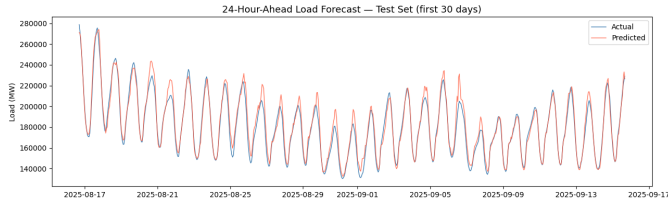


Fig. 2. 24-hour-ahead XGBoost load forecast (red) vs. actual load (blue) for the first 30 days of the test set (Aug.–Sep. 2025). The model achieves MAPE = 2.73% and MAE = 5,340 MW.

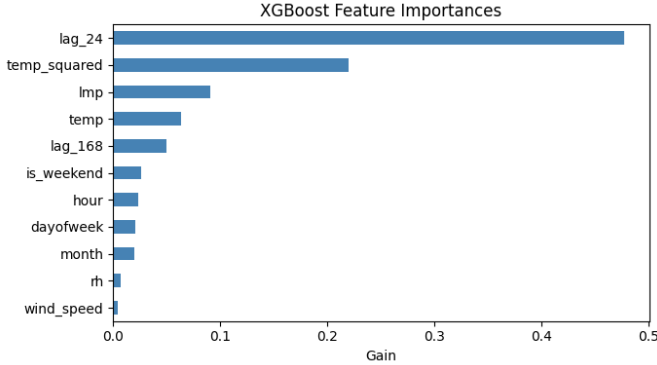


Fig. 3. XGBoost gain-based feature importance. The 24-hour lag dominates (gain ≈ 0.48), followed by the squared temperature term, which captures both heating and cooling load responses.

B. Feature Importance and Stress Identification

Fig. 3 shows XGBoost gain-based feature importance. The 24-hour lag (lag_{24}) is the most influential predictor, with gain ≈ 0.48 , confirming that the previous day’s load at the same hour carries substantial predictive value [10]. The centered quadratic temperature term (temp_squared , gain ≈ 0.22) is the second most important feature because it captures both heating- and cooling-driven demand. DA-LMP (gain ≈ 0.09) and raw temperature (gain ≈ 0.07) follow. The weekly lag (lag_{168}) contributes 0.05, while wind speed and relative humidity contribute little (both below 0.02).

We classify hours with forecast load above the 90th percentile of the training distribution as grid stress hours. We use the 90th percentile rather than the 95th percentile because the higher cutoff would identify only about 258 hours in the test set, which is too sparse to provide meaningful pricing coverage during the fall and winter stress periods in this sample. The 90th-percentile rule identifies 666 stress hours (12.9% of the test set), corresponding to a threshold of 229,127 MW. This threshold lies well above average load while still activating during elevated, though not extreme, fall demand conditions that account for most constrained hours in the test period.

IV. THRESHOLD-BASED PRICING FRAMEWORK

A. Pricing Rule and Constraints

We model the interaction between the grid operator and consumers using a deterministic price-response structure, motivated by the Stackelberg game-theoretic framework [8], [9].

For each hour t , the operator sets a price p_t based on the day-ahead load forecast. Consumers then adjust flexible load according to the following constant-elasticity demand function:

$$L_t(p_t) = L_t^{\text{base}} \cdot \max\left(0, 1 - \varepsilon \cdot \phi \cdot \left(\frac{p_t}{\bar{p}} - 1\right)\right), \quad (1)$$

where L_t^{base} is the day-ahead forecast load, $\varepsilon = 0.30$ is the assumed price elasticity of flexible load, $\phi = 0.45$ is the assumed share of price-responsive load, and $\bar{p} = \$0.12/\text{kWh}$ is the flat-rate reference price.

We set $\varepsilon = 0.30$ based on the residential short-run estimates reported by Mamkhezri [12], which fall in the 0.25–0.35 range. This choice is intended to reflect the concentration of PJM stress hours in evening periods with a largely residential load profile. We set $\phi = 0.45$ as a plausible near-term scenario in which electric-vehicle adoption and smart-device penetration are moderate: higher than the approximately 0.10–0.20 share typical of low-income households without flexible assets [3], [4], but below the 0.60–0.65 share observed in highly electrified households. Both parameters are applied uniformly across the PJM system. This simplification likely overstates curtailment at commercial and industrial nodes, and we revisit this limitation in Section VI.

The pricing rule is subject to three constraints. First, the price cap is set at $P_{\text{max}} = \$0.28/\text{kWh}$, or about 2.3 times the flat rate. This value is intended to limit consumer exposure while still allowing a meaningful stress-period signal. A higher cap, such as $\$0.35/\text{kWh}$, would increase the theoretical maximum reduction in (3), but would also move closer to the bill-shock concerns emphasized by Borenstein [6] and Allcott [4]. The constraints are:

- 1) **Price cap:** $p_t \leq P_{\text{max}} = \$0.28/\text{kWh}$.
- 2) **Price floor:** $p_t \geq P_{\text{min}} = \$0.06/\text{kWh}$.
- 3) **Revenue adequacy:** $\bar{p}_{\text{avg}} \geq \$0.10/\text{kWh}$.

The price floor of $\$0.06/\text{kWh}$ is set at half the flat rate and reflects avoided capacity-cost savings returned to consumers as an incentive to shift discretionary demand. The revenue-adequacy threshold of $\$0.10/\text{kWh}$ is set below the flat rate to give the pricing rule room to operate without immediately binding in periods with relatively few stress hours. If the revenue-adequacy constraint binds, normal peak prices are shifted upward uniformly until the condition is satisfied.

Because $L_t(p_t)$ in (1) is decreasing in p_t , the load-minimizing stress-hour price is the cap, $p_t^* = P_{\text{max}}$. Applying the cap outside stress hours would increase consumer cost without a corresponding system benefit. The resulting three-tier schedule is:

$$p_t^* = \begin{cases} \$0.28/\text{kWh}, & \text{if stress hour,} \\ \$0.12/\text{kWh}, & \text{if peak hour,} \\ \$0.06/\text{kWh}, & \text{if off-peak hour.} \end{cases} \quad (2)$$

Based on (2), a stress hour is any hour with forecast load above 229,127 MW, regardless of time of day. For non-stress hours, peak hours run from 07:00 to 21:59, and off-peak hours

TABLE II
PERFORMANCE COMPARISON OF THREE PRICING SCHEMES (TEST SET)

Metric	Flat	TOU	Proposed
Peak Load (MW)	277,291	272,944	242,750
Peak Red. vs Flat	—	1.6%	12.5%
Bill Savings vs TOU	—	—	11.7%
Bill vs Flat	—	-15.1%	-1.6%
Price Std Dev (\$/kWh)	0.0000	0.0484	0.0673
Price Cap Respected	N/A	N/A	✓
Price Floor Respected	N/A	N/A	✓

Note: Parameters: $\varepsilon = 0.30$, $\phi = 0.45$, $\bar{p} = \$0.12/\text{kWh}$, threshold = 229,127 MW.

run from 22:00 to 06:59. The off-peak price $P_{\min} = \$0.06/\text{kWh}$ is intended to encourage overnight shifting of discretionary loads such as electric-vehicle charging and dishwashing. Under the assumed parameters, the theoretical maximum reduction in stress-hour demand is:

$$\Delta L^{\max} = \varepsilon \cdot \phi \cdot \left(\frac{P_{\max}}{\bar{p}} - 1 \right) = 0.30 \times 0.45 \times \frac{0.16}{0.12} = 18\%. \quad (3)$$

B. Comparison Baselines

1) *Flat-rate*: A constant price of $\bar{p} = \$0.12/\text{kWh}$ with no price signal, so $L_t^{\text{flat}} = L_t^{\text{base}}$.

2) *TOU*: An on-peak price of $\$0.18/\text{kWh}$ during 07:00–21:59 and an off-peak price of $\$0.08/\text{kWh}$ otherwise [2]. Flexible load removed from peak hours is treated as deferred rather than redistributed within the same day, which avoids mechanically creating secondary peaks. The implied TOU shift fraction per peak hour is:

$$\delta_{\text{TOU}} = \varepsilon \cdot \phi \cdot \left(\frac{0.18}{0.12} - 1 \right) = 0.30 \times 0.45 \times 0.50 = 6.75\%. \quad (4)$$

V. SIMULATION RESULTS

A. Summary Results

Table II summarizes the performance of the three pricing schemes across the 5,165-hour test set.

The proposed scheme yields a 12.5% simulated reduction in peak load relative to flat-rate pricing. This outcome is below the 18% theoretical maximum in (3) but substantially larger than the 1.6% reduction under TOU pricing. The weaker TOU result reflects both the smaller peak-to-baseline price differential and the fact that the TOU signal applies uniformly across all on-peak hours rather than only during forecast stress periods.

One exception arises during the December 14–18, 2025 cold snap. In that window, the $\$0.28/\text{kWh}$ stress-hour price produces little visible reduction in aggregate load. Heating-related demand is less flexible than discretionary uses such as

electric-vehicle charging, so the assumed $\phi = 0.45$ flexible-load share likely overstates actual responsiveness during extreme winter conditions. As a result, the effective reduction during that episode was likely smaller than the test-period average implied by the 12.5% headline result. We cannot estimate that difference directly because the PJM data do not provide hour-level end-use decomposition.

B. Load Response During Stress Hours

Fig. 4 shows system load (top) and price signals (bottom) over a representative 10-day window in August 2025. The proposed scheme (blue) reduces peaks that exceed the stress threshold (red dashed line at 229,127 MW), while flat-rate (grey) and TOU (orange) remain more closely aligned. The price panel shows that the proposed scheme reaches $\$0.28/\text{kWh}$ during stress hours and falls to $\$0.06/\text{kWh}$ overnight, whereas TOU alternates between $\$0.18$ and $\$0.08/\text{kWh}$ on a fixed daily schedule independent of grid conditions.

Fig. 5 shows the distribution of system load across the 666 stress hours identified by the forecast rule. Under flat-rate pricing and TOU, the distribution remains concentrated above 220,000 MW, with a long upper tail extending toward 280,000 MW. The proposed scheme shifts the distribution leftward, with its mode near 210,000 MW, or roughly 15,000 MW below the flat-rate mode. This shift is consistent with the reduction implied by the assumed $\varepsilon\phi$ response during stress hours, although the December cold-snap period again appears less responsive than the aggregate distribution suggests.

Fig. 6 plots mean load by hour of day over the full test period. The flat-rate profile (gray circles) peaks near 208,000 MW at 18:00–19:00. TOU (orange squares) lowers evening load but produces a deeper overnight trough ($\approx 172,000$ MW at 03:00). The proposed profile (blue triangles) is the flattest: peak load falls to $\approx 202,000$ MW, and the overnight valley remains higher than TOU’s. The deeper off-peak incentive (0.06 vs. $0.08/\text{kWh}$) attracts flexible load to overnight hours without concentrating it as sharply in the pre-dawn period.

C. Price Variability and Consumer Bills

Fig. 7 shows the price distribution across all 5,165 test hours. Flat-rate pricing is a single mass point at $\$0.12/\text{kWh}$ ($\sigma = 0$). TOU produces two mass points at $\$0.08$ and $\$0.18/\text{kWh}$ ($\sigma = 0.0484$ $\$/\text{kWh}$). The proposed scheme produces across three mass points, $\$0.06$, $\$0.12$, and $\$0.28/\text{kWh}$ ($\sigma = 0.0673$ $\$/\text{kWh}$). Although this implies greater price variation than TOU, the prices are rule-based and observable one day in advance rather than tied to wholesale real-time volatility, which may reduce concerns about bill uncertainty [5]. The right panel confirms that all proposed prices lie within the bounds $[P_{\min}, P_{\max}] = [\$0.06, \$0.28]$ kWh.

Fig. 8 plots the cumulative per-household electricity bill over the seven-month test period. TOU (orange) is the most expensive scheme throughout and finishes 11.7% above the proposed scheme (blue). Flat-rate (gray) lies between the

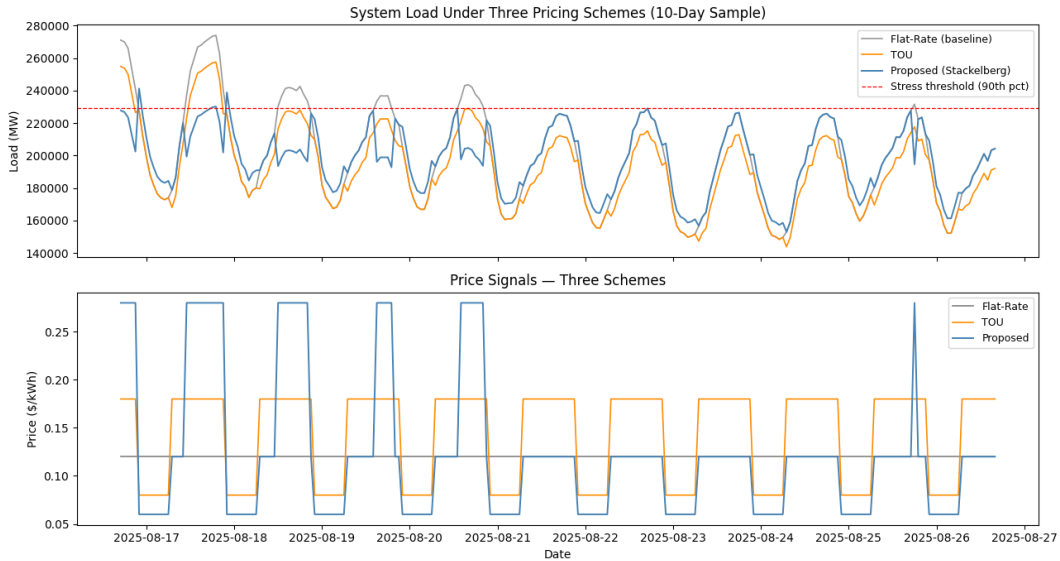


Fig. 4. System load (top) and price signals (bottom) over a 10-day test set sample (Aug. 2025). The proposed scheme (blue) reduces peaks above the stress threshold (red dashed, 229,127 MW) and applies a \$0.06/kWh off-peak price overnight.

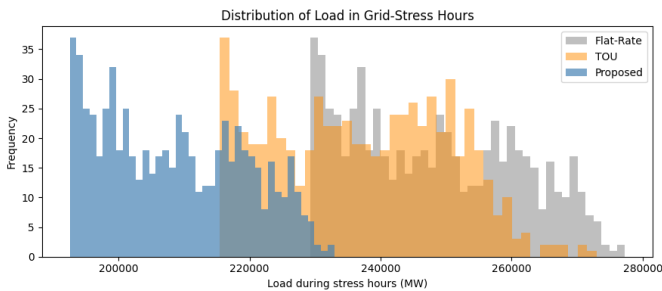


Fig. 5. Distribution of system load during the 666 grid-stress hours (12.9% of the test set). The proposed scheme (blue) shifts load leftward relative to both baselines, with its mode approximately 15,000 MW below the flat-rate mode.

two and ends 1.6% above the proposed scheme. The bill advantage of the proposed scheme comes less from stress-hour curtailment itself than from the lower off-peak price of \$0.06/kWh relative to the TOU floor of \$0.08/kWh. Because most hours in the sample are non-stress hours, the lower off-peak price contributes more to cumulative bill savings than the stress-period premium contributes to bill increases.

VI. DISCUSSION, LIMITATIONS, AND FUTURE WORK

The proposed framework couples a 24-hour-ahead XGBoost forecast (MAPE of 2.73%, MAE of 5,340 MW) with a deterministic three-tier pricing rule subject to a \$0.28/kWh cap, a \$0.06/kWh floor, and a revenue-adequacy constraint. Simulations on the August 2025–March 2026 test set indicate a 12.5% peak demand reduction relative to flat-rate pricing and 11.7% consumer bill savings relative to TOU, contingent on assumed elasticity parameters. The stress-hour price (\$0.28/kWh) drives the peak reduction, while the off-peak discount (\$0.06/kWh) accounts for most of the bill advantage

across the 87.1% of hours that fall outside stress periods. TOU’s mean price (\$0.1425/kWh) exceeds the flat-rate price (\$0.12/kWh) because 15 daily peak hours carry a \$0.18/kWh regardless of actual grid stress. The proposed framework elevates prices only during the 12.9% of hours when stress is forecast, keeping the net mean price competitive.

The 12.5% simulated peak reduction falls short of the 18% theoretical maximum from (3). The 90th-percentile threshold (229,127 MW) captures elevated but not extreme load, so fall stress hours sit well below the 277,000 MW summer peak and produce smaller MW curtailments for the same price signal. The December 2025 cold snap (Dec. 14–18) illustrates this: heating-dominant load reduces the effective flexible-load fraction well below the assumed $\phi=0.45$, and curtailment from a \$0.28/kWh signal in that window was likely negligible in practice.

The uniform $\varepsilon=0.30$ and $\phi=0.45$ applied across PJM’s roughly 65 million people are a simplification of the model. Low-income households are least likely to own EVs, smart thermostats, or programmable appliances, and they probably have effective flexible-load shares closer to $\phi=0.10$ [3], [4]. A two-segment model would shrink the 12.5% aggregate figure and expose a sharper distributional problem: the stress-hour premium falls on all consumers equally, but only flexible households reduce consumption to avoid it. This cannot be corrected without segment-level consumption data that PJM’s aggregate series does not provide.

The hour-by-hour pricing structure ignores battery storage cycling, building thermal inertia, and consumer anticipation. A consumer who pre-cools before a stress event shifts load into the unconstrained window, partially overstating both the reported peak reduction and bill savings. Forecast error near the 229,127 MW threshold introduces a related issue: border-

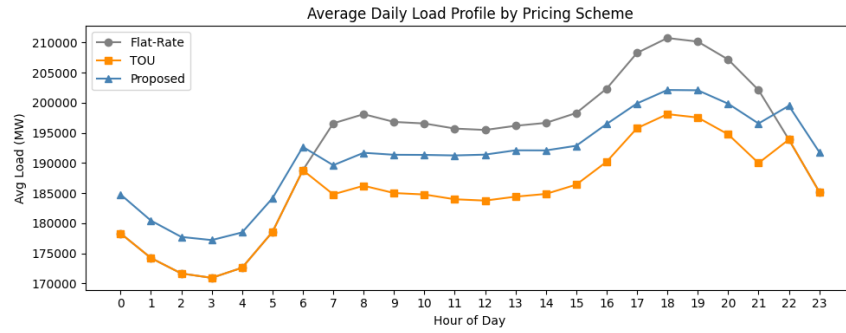


Fig. 6. Average daily load profile by pricing scheme across the full test period. The proposed scheme (blue triangles) produces the flattest profile, reducing the evening peak to $\approx 202,000$ MW while maintaining a higher overnight floor than TOU.

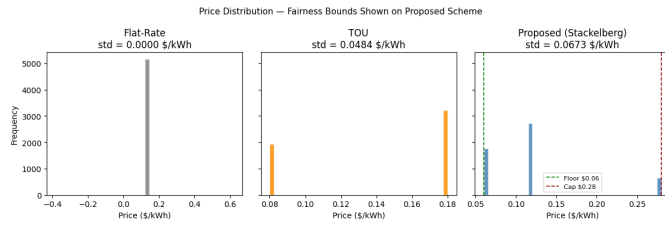


Fig. 7. Price distributions for all three schemes. The proposed scheme's three-tier structure (right panel) is bounded by the price floor ($\$0.06/\text{kWh}$, green dashed) and cap ($\$0.28/\text{kWh}$, red dashed), with all prices within these bounds.

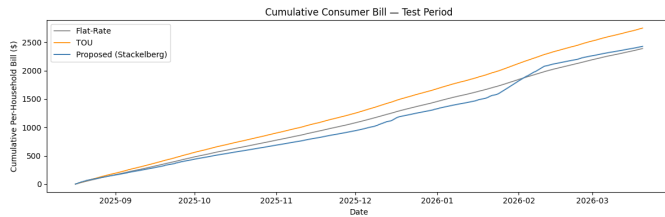


Fig. 8. Cumulative per-household electricity bill over the Aug. 2025 to Mar. 2026 test period under three pricing schemes. The proposed scheme (blue) finishes 11.7% below TOU (orange) and 1.6% below flat-rate (gray), driven primarily by the $\$0.06/\text{kWh}$ off-peak.

line misclassification triggers $\$0.28/\text{kWh}$ prices on unstressed hours. Finally, the price cap and floor bound volatility uniformly across consumers, which constitutes bounded pricing, not equity analysis.

The most immediate extension is replacing the uniform $\varepsilon=0.30$ with segment-specific elasticities [8], [12], which would simultaneously improve aggregate accuracy and surface the distributional effects identified above. A multi-period formulation that tracks battery storage cycling and building thermal inertia is the natural next step. A pricing rule robust to forecast errors in the 225,000–235,000 MW range, for example, a probabilistic threshold or a dead band around the stress boundary, would address borderline misclassification. Over the longer term, extending the test period to cover multiple summers and incorporating segment-level consumption data would enable a more credible evaluation of both efficiency and equity outcomes prior to any pilot deployment.

REFERENCES

- [1] T. Hofmann and M. Lindberg, "Household demand flexibility and dynamic electricity pricing: Evidence from a real-world experiment," *Energy Policy*, vol. 185, Feb. 2024, Art. no. 113821, doi: 10.1016/j.enpol.2023.113821.
- [2] A. Faruqui and S. Serfici, "Household response to dynamic pricing of electricity: A survey of 15 experiments," *Energy J.*, vol. 31, no. 2, pp. 193–217, 2010, doi: 10.5547/ISSN0195-6574-EJ-Vol31-No2-5.
- [3] M. Cahana, N. Fabra, M. Reguant, and J. Wang, "The distributional impacts of real-time pricing," CEPR Discussion Paper No. DP17200, Apr. 2022. [Online]. Available: <https://ssrn.com/abstract=4121375>
- [4] H. Allcott, "Rethinking real-time electricity pricing," *Resour. Energy Econ.*, vol. 33, no. 4, pp. 820–842, Nov. 2011, doi: 10.1016/j.reseneeco.2011.06.003.
- [5] S. Numminen, J. Koponen, and P. Lund, "Barriers to the adoption of dynamic electricity pricing among consumers," *Sustain. Energy Grids Netw.*, vol. 41, Mar. 2025, Art. no. 100210, doi: 10.1016/j.segy.2025.100210.
- [6] S. Borenstein, "The long-run efficiency of real-time electricity pricing," *Energy J.*, vol. 26, no. 3, pp. 93–116, 2005.
- [7] K. Spees and L. B. Lave, "Demand response and electricity market efficiency," *Electr. J.*, vol. 20, no. 3, pp. 69–85, Apr. 2007, doi: 10.1016/j.tej.2007.03.002.
- [8] R. Yu, W. Yang, and S. Rahardja, "A statistical demand-price model with its application in optimal real-time price," *IEEE Trans. Smart Grid*, vol. 3, no. 4, pp. 1734–1742, Dec. 2012, doi: 10.1109/TSG.2012.2210376.
- [9] S. Maharjan, Q. Zhu, Y. Zhang, S. Gjessing, and T. Basar, "Dependable demand response management in the smart grid: A Stackelberg game approach," *IEEE Trans. Smart Grid*, vol. 4, no. 1, pp. 120–132, Mar. 2013, doi: 10.1109/TSG.2012.2223753.
- [10] T. Hong and S. Fan, "Probabilistic electric load forecasting: A tutorial review," *Int. J. Forecast.*, vol. 32, no. 3, pp. 914–938, Jul.–Sep. 2016, doi: 10.1016/j.ijforecast.2015.11.001.
- [11] T. Zhang, Y. Wang, X. Li, J. Chen, H. Liu, Q. Zhao, and Z. Xu, "Long-term energy and peak power demand forecasting based on Sequential-XGBoost," *IEEE Trans. Power Syst.*, vol. 39, no. 2, pp. 3088–3104, Mar. 2024, doi: 10.1109/TPWRS.2023.3273985.
- [12] J. Mamkhezri, "Assessing price elasticity in US residential electricity consumption: A comparison of monthly and annual data with recession implications," *Energy Policy*, vol. 200, Apr. 2025, Art. no. 114539, doi: 10.1016/j.enpol.2024.114539.